JOURNAL OF VIROLOGY, Nov. 1993, p. 6453–6462
0022-538X/93/116453-10$02.00/0

Vol. 67, No. 11

# Molecular and Biochemical Bases for Activation of the Transforming Potential of the Proto-Oncogene c-*ros*

CONG S. ZONG, BETTY POON,† JIANMIN CHEN, AND LU-HAI WANG*

*Department of Microbiology, Mount Sinai School of Medicine, New York, New York 10029-6574*

Received 3 June 1993/Accepted 29 July 1993

**The transforming gene of avian sarcoma virus UR2, v-*ros*, encodes a receptor-like protein tyrosine kinase and differs from its proto-oncogene, c-*ros*, in its 5′ truncation and fusion to viral *gag*, a three-amino-acid (aa) insertion in the transmembrane (TM) domain, and changes in the carboxyl region. To explore the basis for activation of the c-*ros* transforming potential, various c-*ros* retroviral vectors containing those changes were constructed and studied for their biological and biochemical properties. Ufcros codes for the full-length c-*ros* protein of 2,311 aa, Uppcros has 1,661-aa internal deletion in the extracellular domain, CCros contains the 3′ c-*ros* cDNA fused 150 aa upstream of the TM domain to the UR2 *gag*, CVros is the same as CCros except that the 3′ region is replaced by that of v-*ros*, and VCros is the same as CCros except that the 5′ region is replaced by that of v-*ros*. The Ufcros, Uppcros, CCros, and CVros are inactive in transforming chicken embryo fibroblasts, whereas VCros is as potent as UR2 in cell-transforming and tumorigenic activities. Upon passages of CCros and CVros viruses, the additional extracellular sequence in comparison with that of v-*ros* was deleted; concurrently, both viruses (named CC5d and CV5d, respectively) attained moderate transforming activity, albeit significantly lower than that of UR2 or VCros. The native c-*ros* protein has a very low protein tyrosine kinase activity, whereas the ppcros protein is constitutively activated in kinase activity. The inability of CCros and CVros to transform chicken embryo fibroblasts is consistent with the inefficient membrane association, instability, and low kinase activity of their encoded proteins. The CC5d and CV5d proteins are indistinguishable in kinase activity, membrane association, and stability from the v-*ros* protein. The reduced transforming potency of CC5d and CV5d proteins can be attributed only to their differential substrate interaction, notably the failure to phosphorylate a 88-kDa protein. We conclude that the 5′ rather than the 3′ modification of c-*ros* is essential for its oncogenic activation; the sequence upstream of the TM domain has a negative effect on the transforming activity of CCros and CVros and needs to be deleted to activate their biological activity.**

The proto-oncogene c-*ros* is the cellular counterpart of the oncogene v-*ros* of avian sarcoma virus (ASV) UR2 (30, 31). Sequence analysis of the chicken and human genomic DNA clones representing the 3′ portion of c-*ros* revealed that it is a receptor-like protein tyrosine kinase (PTK) (28, 30). Recently, the c-*ros* cDNAs from rat (29), human (3), and chicken (5) have been isolated and sequenced. Those results confirm the initial suggestion that c-*ros* codes for a receptor-like PTK. However, it differs from other well-characterized receptor PTKs (RPTKs) such as the insulin receptor (IR) and insulin-like growth factor I receptor (IGFR) (8, 40, 42), epidermal growth factor receptor (41), platelet-derived growth factor receptor (47), and colony-stimulating factor 1 receptor (6, 17, 46) in that the predicted c-*ros* product has an extraordinary large extracellular (EC) domain (3, 5, 29). Both the sequence and the predicted structure of the c-*ros* product show a remarkable homology with those of the *sevenless* protein of *Drosophila melanogaster* (3, 5, 15, 29). The PTK domain of c-*ros* also shows a close homology with those of IR and IGFR (8, 40, 42).

The normal function of c-*ros* remains unknown. Its expression is very restricted. In chickens, only kidney, intestine, thymus, bursa, and gonad tissues express detectable amount of c-*ros* RNA (5, 6, 30). In rat, aside from kidney, c-*ros* RNA is also expressed in heart, lung, and testis (29). Recent studies of c-*ros* expression by in situ hybridization detected its presence in the developing collecting ducts of kidney and villi of intestine and implicated c-*ros* in epithelial cell differentiation during embryogenesis (6, 37, 39). Besides the spontaneous transduction and activation of the tumorigenic potential of c-*ros* in ASV UR2, there has been a report on activation of the transforming and tumorigenic potential of human c-*ros* in a mammary carcinoma cell line (2). Furthermore, a high percentage of human glioblastoma cell lines surveyed were found to express elevated levels of c-*ros* RNAs, some of which were the products of rearranged c-*ros* gene (4). These observations implicate the involvement of c-*ros* in the development of glioblastomas. However, there have not been reports on c-*ros* expression in fresh tumor tissues.

ASV UR2 codes for a Gag-Ros fusion protein of 68 kDa which is a transmembrane (TM) protein with the *gag* moiety protruding extracellularly (20). The $P68^{gag\text{-}ros}$ is capable of autophosphorylation and phosphorylation of foreign substrates (11, 20). Our earlier mutagenesis studies indicated that the *gag* moiety and membrane association of $P68^{gag\text{-}ros}$ are essential for its transforming activity (21, 22). Comparison of the sequences of v-*ros* and c-*ros* revealed three structural alterations in v-*ros* (Fig. 1A) (5, 30, 31): (i) v-*ros* is truncated 7 amino acids (aa) upstream of the TM domain of c-*ros* and joined in frame to the 5′ *gag* sequence of UR2, (ii) there is a 3-aa insertion in the TM domain of v-*ros*, and (iii) the 3′ sequence of c-*ros* is truncated and modified in v-*ros*. Any one or a combination of these changes from c-*ros* could be responsible for the activation of its transforming potential. To address this question and to explore the underlying biochemical basis, we have constructed retroviruses containing full-length or internally truncated c-*ros* cDNA as well as various v-*ros* and

* Corresponding author.
† Present address: Department of Microbiology, University of California, Los Angeles, CA 90024.

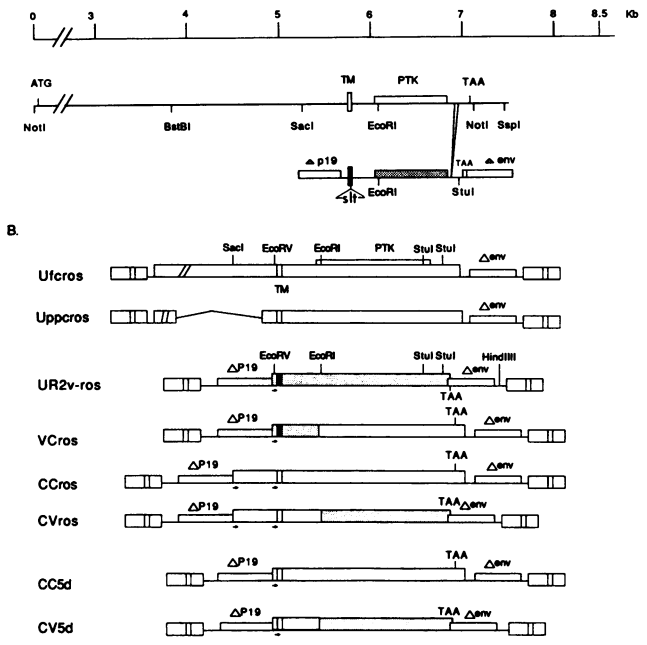


FIG. 1. Constructs of c-*ros* and c-*ros* × v-*ros* recombinant retroviral vectors. (A) The structures of c-*ros* and v-*ros* are shown to scale, with various structural domains, restriction sites, and differences highlighted. The termination codon TAA is indicated; in v-*ros*, it terminates within the viral *env* region. The 3-aa insertion in the TM domain and the 12-aa deletion in the carboxyl region of v-*ros* are indicated (see Fig. 2). (B) The various c-*ros* and recombinant retroviral vectors were constructed by using the indicated restriction sites (see Materials and Methods). Small open boxes denote viral *gag* and *env* sequences; shaded boxes indicate the v-*ros* sequence; large open boxes represent the c-*ros* sequence. The TM domains of c-*ros* and v-*ros* are represented by open and solid boxes, respectively. The ectodomains of Ufcros and Uppcros are interrupted to reflect their actual lengths. The deletion in Uppcros is shown by the two bent lines. The small arrows underlining the EC sequences in CCros and CVros represent 21-nucleotide repeats of the *ros* sequence immediate upstream of the TM domain as a result of the construction. Only one copy of that sequence is present in UR2, VCros, CC5d, and CV5d.

c-*ros* chimeras and analyzed their biological and biochemical activities. Our data show that the 5′ rather than the 3′ modifications in v-*ros* are essential for the activation of c-*ros*. Sequence immediately upstream of the TM domain appears to exert a negative effect on the transforming ability of the c-*ros*-containing viruses, apparently as a result of its effect on the stability, membrane association, and kinase activity of the Gag-Ros proteins. The nontransforming CCros and CVros chimeras gave rise to moderately transforming derivatives apparently by deleting the c-*ros*-derived EC sequences. The weak transforming potency of these variants in comparison with UR2 does not correlate with the kinase activity but instead correlates with differential cellular substrate interactions. These variants are potentially invaluable for identifying cellular proteins involved in the process of cell transformation.

## MATERIALS AND METHODS

**Cells and viruses.** The preparation and maintenance of chicken embryo fibroblasts (CEF) and the colony formation assay of virus-infected cells were carried out by published procedures (18). ASV UR2 and its associated helper virus UR2AV have been described elsewhere (31, 45). For Rous sarcoma virus (RSV), the subgroup A Schmidt-Ruppin strain was used.

**Construction of fcros and ppcros expression plasmids.** Three previously described overlapping c-*ros* cDNA clones, 5b, 10a, and 84-1 (in 5′-to-3′ order) (5), were used to construct the full-length c-*ros* cDNA in plasmid pBluescript SK(+) or SK(−) (Stratagene). This was done by using the unique *Bst*BI sites in clones 5b and 10a and the unique *Sac*I sites in the 3′ ends of 10a and 84-1 to form the full-length cDNA, which was subcloned at the *Sal*I site of the vector. Most of the 5′ and 3′ noncoding sequences of the resulting full-length cDNA was then deleted by using the polymerase chain reaction (PCR) method with a pair of synthesized oligodeoxynucleotides each containing a *Not*I site. The resulting plasmid was named pSKcros.

For transient expression of c-*ros* in COS 7 cells, pECE vector (9) containing the simian virus 40 early promoter, replication origin, and polyadenylation signal was used. The replication origin allows the transfected plasmid DNA to be amplified in COS cells expressing the simian virus 40 T antigen (9). The 7-kb full-length c-*ros* was freed from pSKcros by *Not*I digestion and inserted into a modified pECE vector containing a *Not*I site, resulting in pEfcros. The deletion variant ppcros was initially engineered in pSKcros by deleting 4,983 nucleotides of the EC sequence flanked by *Pst*I and *Pvu*II sites to produce pSKppcros. The ppcros sequence was then excised from pSKp pcros by *Not*I digestion and inserted into the expression vector pRCMV (Invitrogen) under the control of the human cytomegalovirus early promoter and enhancer. The resulting plasmid was named pCMVppcros.

For expression of c-*ros* proteins in CEF, the full-length c-*ros* and ppcros were introduced individually into pUIGFRΔATG, in which the *gag* initiation codon was mutated (26, 27). The resulting plasmids are called pUfcros and pUppcros, respectively. These plasmids encode the full-length or 5′ internally deleted c-*ros* protein, using its native initiation codon. The c-*ros* sequence is flanked by the viral long terminal repeats in these vectors and can be transfected directly into CEF for their expression (27).

**Construction of c-*ros* and v-*ros* recombinants.** Chicken c-*ros* cDNA clone 84-1, containing the 3′-most 3,000 nucleotides (5), and pUR2HI, containing the entire UR2 genome cloned in pBR322 and permuted at the *Hin*dIII site (31), were used. pUR2H1 was digested completely with *Stu*I and then partially with *Eco*RI (there is another *Eco*RI site in the pBR322 DNA downstream of the UR2 genome) to remove the 3′ v-*ros* sequence downstream of the *Eco*RI site (Fig. 1B). The resulting 7.1-kb *Eco*RI-to-*Stu*I pUR2HI plasmid DNA retaining only the 5′ v-*ros* sequence upstream of the *Eco*RI site was ligated to the 0.9-kb *Eco*RI-to-*Ssp*I 3′ c-*ros* fragment (Fig. 1A) to generate pVCros. An intermediate plasmid, pCC3d, was prepared for the construction of pCCros and pCVros. pCC3d was generated by inserting the 1.8-kb *Sac*I-*Ssp*I c-*ros* DNA fragment (Fig. 1A) into the *Eco*RV and *Cla*I sites of pUR2HI, replacing its original sequence. The *Cla*I site is 3′ to the UR2 genome and immediately upstream of the *Eco*RI site in pBR322. As a result, the entire v-*ros* sequence, except the 7 aa upstream of the *Eco*RV site, and the 3′ viral *env* sequence in pUR2H1 are replaced by the 1.8-kb c-*ros* sequence. pCC3d was then completely digested with *Eco*RI to remove the 0.9-kb fragment containing the 3′ c-*ros* and some pBR322 sequences. The resulting 6.4-kb plasmid DNA was ligated with the 0.9-kb *Eco*RI (located in the *ros*)-to-*Eco*RI (located in pBR322) DNA fragment derived from pUR2HI or pVCros to create pCVros or pCCros, respectively (Fig. 1B). The 0.9-kb *Eco*RI-

*Eco*RI DNA fragment not only provides the 3′ *ros* sequence but also restores the 3′ viral sequences lacking in the 6.4-kb plasmid DNA.

**Construction of mammalian expression vectors for CCros and CVros.** pCCros and pCVros DNAs were digested with *Cla*I completely to linearize the plasmids and then ligated to a *Cla*I-*Xba*I oligonucleotide linker. The ligation products were digested partially with *Sac*I, and the 3-kb CCros and 2.9-kb CVros *Sac*I-to-*Xba*I DNAs were isolated. These DNA fragments containing the entire Gag-CCros or Gag-CVros coding sequence were ligated to *Sac*I- and *Xba*I-digested pECE to obtain pECCros and pECVros, respectively.

**Cloning and sequencing of CC5d and CV5d DNAs.** CC5d and CV5d are transforming variants derived from the parental nontransforming CCros and CVros constructs, respectively (see above). Total DNAs were isolated from CC5d- and CV5d-infected CEF (30, 31). The upstream primers used for PCR were 5′ (353)GTGATTCTGGTCGCCCGG(370) 3′ and 5′ (539)ATCACTGCGGCGCTCTCCC(557) 3′, and downstream primers were 5′ (866)GCTGTGATTGGAGCAGT (882) 3′ (upstream of the TM domain) and 5′ (942)GATGAA ATCCCAGAAAA(958) 3′ (downstream of the TM domain). The numbers in parentheses indicate the nucleotide positions of the published UR2 sequence (31). The latter primer has the advantage of allowing us to confirm the CC5d and CV5d DNAs clones by their c-*ros*-derived TM domains as a result of the lack of a 3-aa insertion compared with that in v-*ros*. PCR was carried out according to the procedure described previously (23). The PCR products were cloned into pBluescript SK(+) (Stratagene) and sequenced by the dideoxynucleotide method (36).

**DNA transfection and RNA analysis.** DNA transfection and Northern (RNA) analysis of viral RNAs were performed by published methods (24, 44). For transfection of COS cells, either the calcium phosphate (14) or electroporation method was used. Chloroquine (100 μM) was added immediately after addition of DNA precipitates to cells, and dimethyl sulfoxide shock was omitted in the calcium phosphate method. For electroporation, $1.5 \times 10^6$ cells were suspended in 0.35 ml of phosphate-buffered saline (PBS); then 5 to 10 μg of DNA was dissolved in 50 μl of PBS and added to the cell suspension. The mixture was placed on ice for 5 min and then subjected to electroporation at 300 V and 125 capacitance in a gene pulser apparatus (Bio-Rad). Cells were then placed on ice for another 5 min before plating onto culture dishes.

**Protein analysis.** Metabolic labeling, protein extraction, subcellular fractionation, immunoprecipitation, sodium dodecyl sulfate (SDS)-polyacrylamide gel electrophoresis, and in vitro kinase assays were done according to published procedures (11, 13–20, 22). For glycosylation-inhibiting experiments, cells were pretreated with tunicamycin (10 μg/ml; Sigma) for 2 h and then [$^{35}$S]methionine labeled for 4 h in the presence of tunicamycin. For transiently expressed proteins in COS cells, labeling was carried out 48 h after transfection. Polyclonal antiserum 4-263, recognizing the kinase region of v-*ros* (23), was used for immunoprecipitation and Western blot (immunoblot) analysis of cell lysates as described previously (13, 16), with slight modifications (21, 22). A polyclonal antiphosphotyrosine (anti-P-Tyr) antibody raised against the copolymer of phosphotyrosine, alanine, and glycine has been described elsewhere (23). Monoclonal anti-P-Tyr antibodies PY20 and 4G10 were purchased from ICN and UBI, respectively.

**Detection of cell surface protein.** Virus-infected CEF were washed with PBS three times. The cells were then put on ice and labeled with 0.5 mM sulfo-*N*-hydroxysuccinimide-Biotin (Sigma) for 2 h with occasional mixing. After the biotin solution was removed, the cells were washed three times with F10 medium containing 5% calf serum and three times with Tris-glucose buffer (27); then proteins were extracted by using radioimmunoprecipitation assay buffer and immunoprecipitated with anti-Ros as described above. After Western blotting, the proteins were detected by color development as follows. The filter was blocked by incubation in Tris-buffered saline (20 mM Tris-HCl, 150 mM NaCl, 0.05% Tween 20, 0.02% azide) containing 5% albumin for 1 h at room temperature and then reacted with avidin-alkaline phosphatase (Boehringer Mannheim) in Tris-buffered saline containing 1% albumin for 1 h. After being washed with Tris-buffered saline three times, the filter was immersed briefly in color-developing solution (100 mM Tris-HCl [pH 9.5], 100 mM NaCl, 5 mM $MgCl_2$) and then incubated in the same solution containing nitroblue tetrazolium and 5-bromo-4-chloro-3-indolylphosphate (Promega) for an appropriate period of time at room temperature. The reaction was stopped by rinsing the filter in water.

## RESULTS

**Differences in v-*ros* and c-*ros* sequences.** On the basis of the UR2 v-*ros* and c-*ros* genomic DNA sequences, we showed that v-*ros* differs from c-*ros* in the TM domain and the carboxyl end (Fig. 1A) (30, 31). After sequencing the 3′ c-*ros* cDNA (5), we found that there was one additional base difference at the 3′ region of v-*ros*. However, we discovered later that this was due to an error in the 3′ v-*ros* sequence published previously (31) by misreading of a compressed CC sequence as C at position 2003 (31). We have resequenced v-*ros* and confirmed that the sequence at position 2003 should be CC. With this correction, the C-terminal amino acid sequence of v-*ros* is as shown in Fig. 2. In addition, we have identified the 3′ v-*ros* sequence downstream of position 1999 that we previously indicated as of unknown origin (31) to be part of the 3′ c-*ros* cDNA sequence (5). There is a deletion of 36 nucleotides between positions 1999 and 2000 of v-*ros* in comparison with c-*ros* cDNA (5). The v-*ros* and c-*ros* sequences are colinear after this in-frame deletion until the 3′ truncation in v-*ros*, where it joins the *env* sequence. At the recombination junction of c-*ros* and *env*, there is a seven-nucleotide stretch of sequence identity (31, 38) (Fig. 2). This sequence could mediate the recombination. As a result, the carboxyl 9 aa of c-*ros* are deleted in v-*ros*, and the reading frame of v-*ros* extends into *env* and terminates 45 nucleotides in *env* with a −1 frame relative to that of the viral gp37 *env* sequence (38). Therefore, the differences of 3′ v-*ros* from c-*ros* include an internal 12-aa deletion, a carboxyl 9-aa truncation, and the addition of a 16-random-aa sequence. The overall differences between c-*ros* and v-ros are (i) 5′ truncation and fusion to *gag*, (ii) 3-aa insertion in the TM domain of v-*ros*, and (iii) 3′ sequence changes (Fig. 1A).

**Construction of c-*ros* and c-*ros* × v-*ros* expression vectors.** To test the transforming potential of c-*ros* and the effect of sequence alterations in v-*ros* on the transforming activity of c-*ros*, we constructed the c-*ros* and c-*ros* × v-*ros* viruses shown in Fig. 1. Ufcros and Uppcros encode c-*ros* proteins from the native initiation codon and contain no *gag* sequences. All of the c-*ros* × v-*ros* chimeras have the same *gag* sequence; however, CCros and CVros contain an additional 526 nucleotides of the EC domain of c-*ros* in comparison with VCros and UR2. The only difference between UR2 (VVros) and VCros, and also between CCros and CVros, is the 3′ alteration in v-*ros* (Fig. 1). Likewise, the only difference between UR2 (VVros) and CVros, and also between VCros and CCros, is in the 5′ region of v-*ros*.

**Transforming potential of c-*ros* viruses.** The pUfcros and

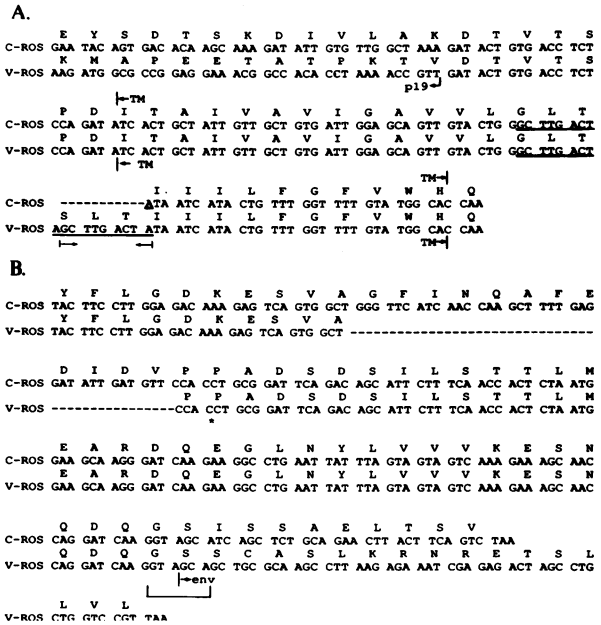


FIG. 2. Differences between c-*ros* and v-*ros*. (A) V-*ros* differs from c-*ros* in its 5′ truncation and joining to the viral p19 *gag* sequence, as indicated by the arrow. The TM domains of c-*ros* and v-*ros* are shown and bounded by the arrows. There is an additional 3-aa segment (SLT) within the TM domain of v-*ros* due to a nine-nucleotide repeat, indicated by the underlined sequence. (B) In the carboxyl region, v-*ros* contains a 12-aa internal in-frame deletion (shown by the broken line) and is fused at its 3′ end to the viral *env* sequence. The CC marked by an asterisk represents the correction to the previously reported v-*ros* sequence (see Results), and the ensuing reading frame is corrected for the error. There is a common seven-nucleotide stretch at the junction of v-*ros* and *env* (bracketed sequence) that is shared by c-*ros* and *env* and may account for the 3′ recombination. This results in deletion of 9 aa from the carboxyl tail of c-*ros* and addition to v-*ros* of 16 novel aa derived from *env*.

pUppcros DNAs contain the nonpermuted viral genome flanked by two long terminal repeats and thus can be used for transfection directly (27). For UR2 and the recombinants whose genomes were permuted at the *Hin*dIII site in the plasmids (30, 31), the viral DNA inserts were freed of plasmid pBR322 by *Hin*dIII digestion, purified, and briefly self-ligated to form nonpermuted viral genomes before transfection. Equal molar amounts of DNA from the various viruses were individually transfected into CEF together with a one-fifth molar amount of helper virus UR2AV DNA, which provided the necessary replicative functions. Within 2 weeks of transfection, VCros- and UR2-transfected CEF were highly elongated and refractile, while Ufcros-, Uppcros-, CCros-, and CVros-transfected cells showed little morphological change in comparison with uninfected CEF (data not shown). We conclude that native c-*ros* and its 5′ internally deleted mutant are unable to transform CEF. The 5′ truncation and fusion to *gag*, neither alone (in CCros) nor in combination with the 3′ change (in CVros), is able to activate the transforming potential of c-*ros*. By contrast, 5′ alteration alone (in VCros) is able to confer to c-*ros* full cell-transforming and tumorigenic activity (see below). The CCros protein has an additional 175 aa in the EC domain and lacks the 3-aa insertion in the TM domain in comparison with VCros protein. These two changes, either alone or in combination, must be responsible for the differential transforming abilities of these proteins.

**Analysis of c-*ros* and c-*ros* × v-*ros* proteins.** Analysis of the nontransforming c-*ros* proteins in transfected CEF was hampered by their very low level expression, as we observed previously for the defective nontransforming variants of UR2 (21, 22). We therefore transferred the coding sequences of Ufcros, CCros, and CVros individually into a simian virus 40-based vector pECE (9) and that of Uppcros into the cytomegalovirus vector pRCMV (see Materials and Methods). Their proteins were analyzed in transiently transfected COS cells. Plasmid pEUR2, which encodes the UR2 P68$^{gag\text{-}ros}$ (22), was analyzed in parallel. The c-*ros* plasmid and its recombinant plasmids expressed the expected c-*ros* proteins, which appeared to be glycosylated, as evidenced by the effect of tunicamycin treatment (Fig. 3C and 4B). The native c-*ros* had

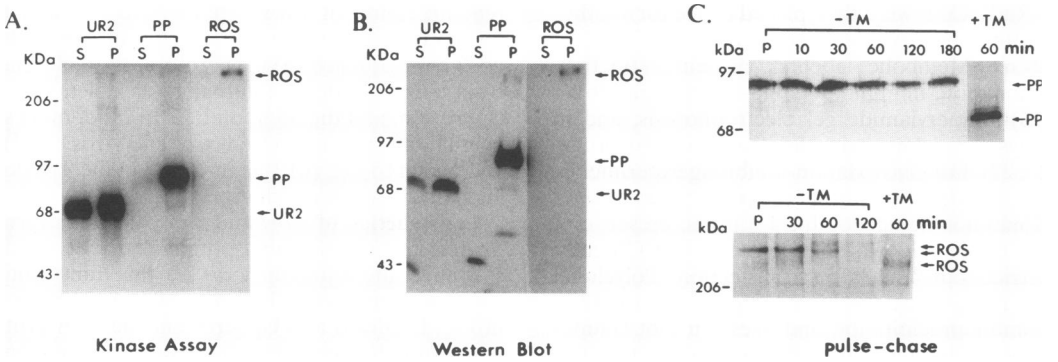


FIG. 3. Analysis of the fcros and ppcros proteins. Twenty micrograms of pEfcros or pCMVppcros was transfected into 4 × 10$^6$ COS 7 cells per 10-cm-diameter dish; 48 h later, the cells were either labeled or extracted directly for protein analysis. (A and B) Kinase activity and abundance of the c-*ros* proteins. Equivalent amounts of unlabeled cell extracts from c-*ros* vector-transfected cells were immunoprecipitated with anti-Ros and divided into duplicates; one aliquot was subjected to in vitro kinase assay by autophosphorylation (A), and the other aliquot was analyzed by Western blotting with anti-Ros for assessing the protein amount (B). The native c-*ros*, ppcros, and UR2 P68$^{gag\text{-}ros}$ proteins are indicated as ROS, PP, and UR2, respectively. S and P stand for S100 and P100 fractions, respectively. The c-*ros* protein lanes in panels A and B were exposed six and three times longer, respectively, than the other lanes. (C) Stability of the c-*ros* proteins. pCMVppcros (top)- or pEfcros (bottom)-transfected cells were pulsed for 20 min with [$^{35}$S]Met (lane P) and chased for the indicated periods of time. Tunicamycin (TM) treatment was done as described in Materials and Methods except that cells were pulsed for 20 min and chased for 60 min. The c-*ros* protein gel was exposed three times longer than the ppcros gel.

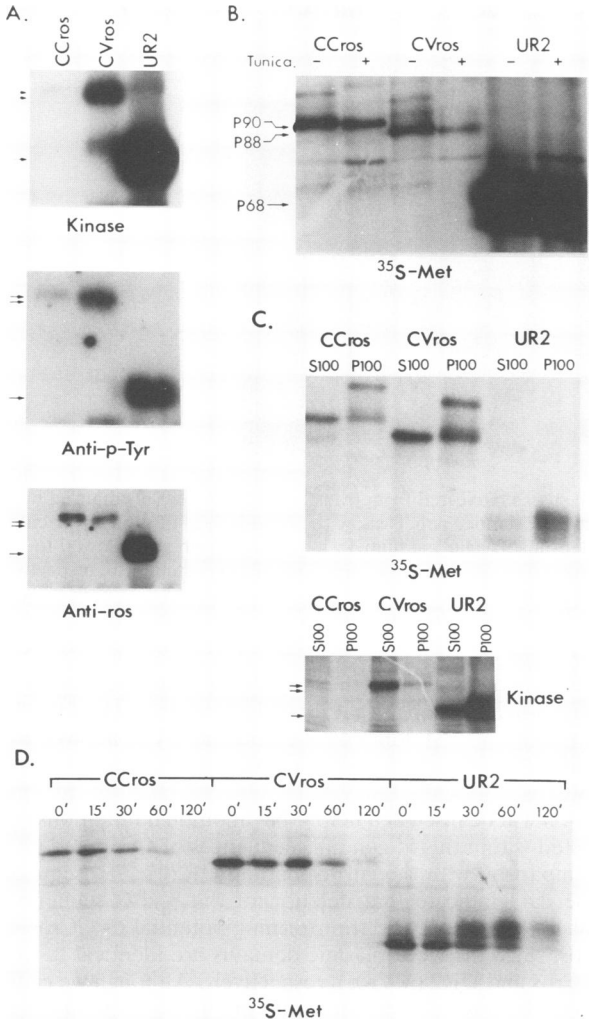


FIG. 4. Analysis of CCros and CVros proteins. Twenty micrograms of pECCros, pECVros, and pEUR2 (22) was transfected into $4 \times 10^6$ COS 7 cells per 10-cm-diameter dish; 48 h later, the cells were either labeled or extracted for protein analysis. In all cases, equivalent amounts of DNA and cells were used for each virus. (A) Kinase activity of the viral proteins. Cell extracts from three dishes were divided into triplicate aliquots and immunoprecipitated with anti-Ros. The immunoprecipitates were subjected to in vitro kinase assay by autophosphorylation (top) or Western blotting either with anti-P-Tyr antibody PY20 (middle) or anti-Ros (bottom). (B) Effect of tunicamycin treatment on the viral proteins (see Materials and Methods for details). (C) Membrane association of the viral proteins. Cells were labeled with [$^{35}$S]Met and analyzed (top). Unlabeled cells were similarly fractionated, immunoprecipitated, and assayed for kinase activity (bottom). (D) Stability of the viral proteins. The transfected cells were pulsed with [$^{35}$S]Met for 20 min and chased for the indicated periods of time (in minutes). Proteins were extracted, immunoprecipitated with anti-Ros, and analyzed.

a very low steady-state protein level and PTK activity (Fig. 3A). By contrast, ppcros protein was much more abundant and had a kinase activity similar to that of UR2 v-*ros*. Most of the c-*ros* and ppcros proteins were associated with the membrane-rich fraction, as was their PTK activity (Fig. 3A and B). The $T_{1/2}$ of ppcros was over 3 h, as opposed to about 1 h for c-*ros* (Fig. 3C). The inability of c-*ros* to transform CEF could be attributed to its low-level expression and weak kinase activity. However, the reason for the failure of ppcros to transform CEF is unclear. Similar to the native c-*ros*, CCros and CVros had a very low steady-state protein level that was apparently due to their instability (Fig. 4D). The in vitro kinase activity and extent of intracellular phosphorylation of CCros and CVros proteins were much lower than those of the UR2 protein (Fig. 4A). Moreover, the CCros and CVros proteins could not associate with the membranes efficiently, since about 50% of the proteins remained in the cytosolic fraction (Fig. 4C). By contrast, association of the v-*ros* protein with membranes was very efficient (Fig. 3B and 4C), and this association had been shown to be cotranslational (13, 22). Surprisingly, very little kinase activity could be detected for the membrane-bound CCros and CVros proteins (Fig. 4C). Most of the kinase activity of CCros and CVros was detected in the cytosolic fraction, albeit at a much lower level than that of v-*ros*. The vast majority of the v-*ros* protein was membrane bound, and its kinase activity could be readily detected (Fig. 3A and 4C). Certain properties of the CCros and CVros proteins, including instability, inefficient membrane association, low kinase activity, and inactivity of the membrane-bound proteins, most likely account for their lack of cell transformation ability.

**Generation of transforming variants CC5d and CV5d.** Four to five weeks or five to six passages after transfection, the CCros- and CVros-transfected cells began to exhibit significant morphological alterations, although they never reached the degree of refractivity exhibited by VCros- or UR2-transfected cells. This phenomenon suggested the emergence of transforming variants from CCros and CVros by further mutation(s), and these variants were named CC5d and CV5d, respectively. Those observations were reexamined by infecting CEF with virus stocks collected 8 weeks after transfection with CCros and CVros, when the cells appeared uniformly transformed. The virus concentration was estimated by slot blot analysis of the viral RNAs, and an equal amount of virus was used to infect CEF. Again, VCros and UR2 were indistinguishable in their cell-transforming activity and were significantly more potent than CC5d and CV5d. Five to ten times fewer colonies were formed by CC5d- or CV5d-infected CEF than by VCros- or UR2-infected cells (Fig. 5 and other data not shown). CV5d, although less potent than VCros and UR2, was more efficient than CC5d (Fig. 5), suggesting that the 3′ change was able to augment the activity to some extent.

To determine the tumorigenicity of c-*ros* viruses, we injected an equivalent amount of each virus into wing webs of 2- to 4-day-old chicks (Table 1). All of the viruses were 100% effective in inducing tumors. Surprisingly, CV5d was nearly as sarcomagenic as VCros and UR2 despite its delay and attenuated activity in cell transformation. The paradox of weak cell-transforming activity and potent tumorigenicity of CV5d will be discussed later. The tumors were apparent within 2 weeks of injection and grew rapidly. They were typical fibrosarcomas and exhibited frequent metastasis into the liver, lungs, kidneys, and bursas when chickens were dissected 4 weeks after injection. CC5d caused tumors in a slower and less virulent manner. Small tumors were noticed 3 to 4 weeks after injection and grew slowly such that the chickens never succumbed to the tumors. Even after 2 months, the tumors never reached the size of VCros-, UR2-, or CV5d-induced tumors. Upon sacrifice and dissection, CC5d-injected chickens did not show metastasis of tumors into other organs.

**Analysis of the CC5d and CV5d genomes.** To identify the molecular basis for activating the transforming activity of CCros and CVros, we analyzed the genomes of CC5d and CV5d. By Northern analysis, CC5d- and CV5d-infected cells were found to synthesize a single 3.4-kb RNA species comi-

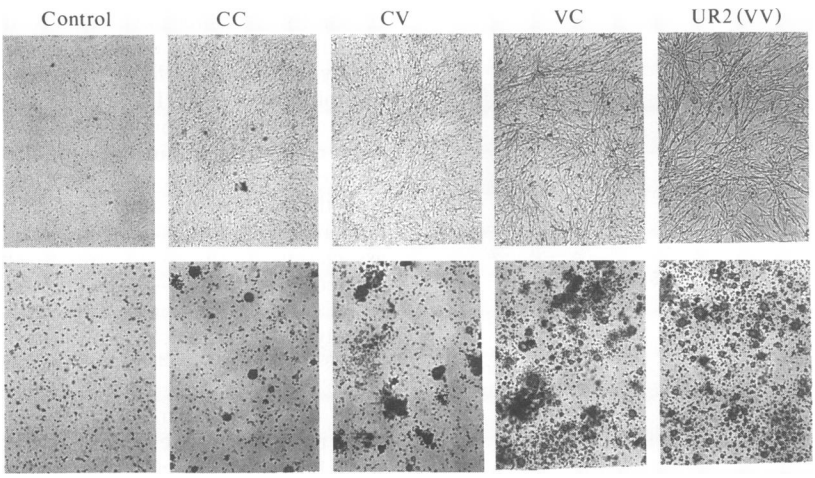


FIG. 5. CEF-transforming activity of c-*ros* × v-*ros* recombinant viruses. Viral stocks harvested from transfected CEF were normalized by slot blot analysis of viral *ros* RNAs. Equivalent amounts of virus were used to infect CEF. Upper panels show the morphology of monolayer culture 4 days after infection; lower panels show the colony-forming ability of cells plated in soft agar medium 15 h after infection and allowed to grow for 10 days. CC and CV represent CC5d and CV5d virus stocks obtained after several passages of CCros- and CVros-transfected CEF, respectively. Similar results were obtained with use of colony-purified CC5d and CV5d virus stocks.

grating with that of UR2, as detected with a v-*ros* probe derived from the kinase domain (data not shown). Since CCros and CVros genomes should be 526 nucleotides larger than the UR2 RNA (Fig. 1) and no RNA of the expected size was detected in CV5d- or CC5d-transformed cells, CCros and CVros had apparently undergone some deletion(s) to generate CC5d and CV5d. Hybridization of the CC5d and CV5d RNAs with probes specific for various regions of the c-*ros* cDNA indicated that most of the EC c-*ros* sequences in the original CCros and CVros constructs were deleted (data not shown). To identify precisely the presumed deletion(s) in CC5d and CV5d, we cloned and sequenced the 5′ fragments of their proviral DNAs by PCR amplification (see Materials and Methods); 32 and 24 independent clones from different PCRs of CC5d and CV5d proviral DNAs, respectively, were analyzed. Sequencing data for those clones containing the 5′ 620-nucleotide DNA fragments of the CC5d and CV5d genomes revealed that they all had undergone identical deletions of 526 nucleotides from the original CCros and CVros constructs. The deletion removed all of the EC sequence except 21 nucleotides upstream of the TM domain and generated the same *gag-ros* junction as that in the UR2 v-*ros*. Lack of the 3-aa insertion in the TM domains of CC5d and CV5d allowed us to positively identify them and to exclude the possibility of UR2 or VCros contamination. A possible mechanism for their deletion will be discussed below. No additional mutations were detected within this 5′ genomic sequences of CC5d and CV5d in comparison with the corresponding UR2 *gag-ros* sequence. These data indicate that deletion of the 5′ EC sequence is sufficient to activate the transforming potential of CCros and CVros, since their cytoplasmic domains are identical to those of VCros and UR2 (VVros), respectively. Although we cannot exclude the possibility of some mutation(s) other than the EC deletion present in CC5d and CV5d, such mutation apparently is unnecessary because VCros has no changes in its cytoplasmic domain in comparison with that of c-*ros*.

TABLE 1. Tumorigenicity assay of c-*ros* recombinant viruses[a]

| Days after injection | Tumor growth ($cm^3$) | | | |
|---|---|---|---|---|
| | CC5d | CV5d | VC | UR2 |
| 14 | 0 | 0.25 | 1.10 | 0.60 |
| 20 | 0.02 | 7.60 | 9.80 | 7.10 |
| 23 | 0.10 | 13.0 | 12.6 | 10.2 |
| 28 | 0.40 | | 26.2 | 21.7 |
| 36 | 2.10 | | | |
| 42 | 5.55 | | | |
| Latency (days) | 21 | 14–20 | 14 | 14 |

[a] An equivalent amount of each virus was injected into the wing webs of 2- to 4-day-old chicks (four chicks per virus in each experiment). The result was pooled from two independent injections. The relative amounts of viruses were determined by slot blot analysis of the viral RNAs extracted from 8 ml of each virus stock, using a *ros*-specific probe. The incidence of tumor induction was 100% in all cases. Tumor growth is expressed as tumor volume per site of injection. The majority of CV5d-, VC-, and UR2-injected chicks did not survive beyond 28 days; a few surviving chicks were sacrificed at that time.

**Analysis of the CC5d, CV5d, and VCros proteins.** To explore the biochemical basis for the different transforming potentials of CC5d and CV5d versus VCros and UR2, we examined the proteins encoded by these viruses. CC5d- and CV5d-infected CEF produced multiple proteins of about 66 to 74 kDa recognized by anti-Ros instead of the 87-kDa protein expected from the CCros and CVros constructs (Fig. 6). This result is consistent with the RNA and sequencing data for CC5d and CV5d. The multiple protein bands (Fig. 6A) were apparently due to posttranslational modification, including phosphorylation and glycosylation (data not shown). Sequencing of the *gag* and EC sequences of the CC5d and CV5d genomes revealed no typical N-linked glycosylation sites. The exact nature of the apparent glycosylation is now under investigation. The heterogeneity of the CC5d and CV5d proteins was not due to mixture of viruses with different deletions, since biologically purified viruses derived from single colonies also gave rise to identical patterns of multiple protein bands. As expected, VCros codes for a P69 *ros* protein which is expected to be 6 aa larger than the P68 of UR2 (Fig. 6). All c-*ros* recombinants and UR2 proteins were capable of in vitro autophosphorylation and phosphorylation of an exogenously added substrate, a bacterial lysozyme polypeptide fragment (25) (Fig. 6B and C). When the autoradiographs were subjected to densitometry

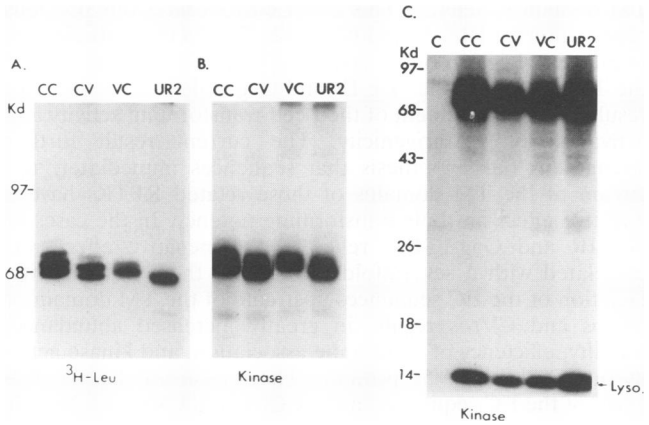


FIG. 6. Protein analysis of c-*ros* × v-*ros* recombinant viruses. Protein extracts from equal numbers of [$^3$H]Leu-labeled infected CEF were divided into triplicate aliquots and subjected to direct immunoprecipitation with anti-ros (A) or in vitro kinase assay following immunoprecipitation without (B) or with (C) 1 μg of exogenously added bacterial lysozyme carboxyl polypeptide fragment. CC, CV, and VC represent CC5d, CV5d, and VCros, respectively; C represents uninfected CEF.

tracing and the values for the kinase assay were adjusted for protein amount, no significant difference in specific PTK activity was founded (Fig. 6 and other data not shown). Therefore, the difference in transforming and tumorigenicity among the viruses cannot be accounted for by different PTK activities of the *ros* proteins.

We next examined the stability of the c-*ros* chimera proteins. The VCros protein was found to have a half-life similar to that of UR2 P68$^{gag\text{-}ros}$, which is about 30 to 40 min (20). By contrast, the half-lives of CC5d and CV5d are somewhat longer; in particular, the $T_{1/2}$ of the CC5d protein appears to be more than 60 min (Fig. 7). Because P68$^{gag\text{-}ros}$ is a membrane-bound protein (20), we examined the possible effect of the 3-aa difference in the TM domain of c-*ros* proteins on their membrane association. Our data showed that like UR2 v-*ros* and VCros proteins, which contained the 3-aa insertion, the vast majority of the CC5d and CV5d proteins lacking the 3-aa insertion were associated with membrane-rich fractions of infected cell extracts (Fig. 8A). The kinase activity was also associated mostly with the membrane-bound proteins. Using biotin labeling of cell surface proteins, we found CC5d and CV5d proteins to be expressed on the cell surface as abundantly as the UR2 protein was (Fig. 8B). The UR2 P68$^{gag\text{-}ros}$ was previously shown to be associated with phosphatidylinositol 3′ kinase (PI3K) activity (12). We also examined the association of c-*ros* chimeric proteins with PI3K. Our data showed that there was no significant difference among the CC5d, CV5d, VCros, and v-*ros* proteins in the ability to associate with the PI3K activity (data not shown). Therefore, the weaker transforming potency of CC5d and CV5d cannot be attributed to the instability, differential subcellular localization, or association with PI3K of their encoded proteins.

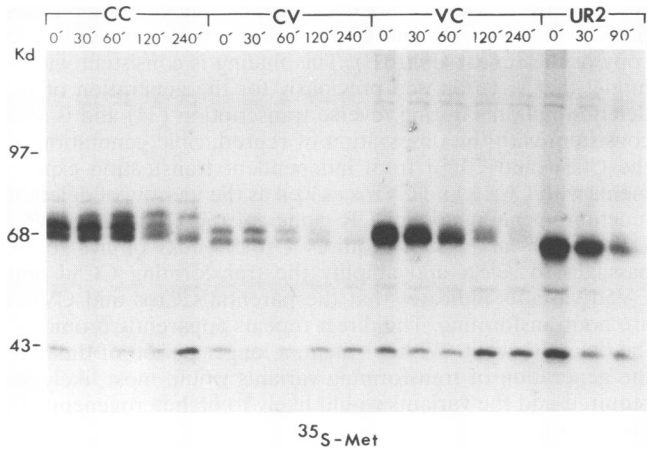


FIG. 7. Stability of the c-*ros* recombinant proteins. Infected CEF were pulsed with [$^{35}$S]Met for 20 min and then chased for the time periods indicated (in minutes). Total proteins were extracted, immunoprecipitated with anti-Ros, and analyzed on an SDS–9% polyacrylamide gel. The 40-kDa protein apparently is a cellular protein precipitated by either protein A or our anti-Ros serum. CC, CV, and VC represent CC5d, CV5d, and VCros, respectively.

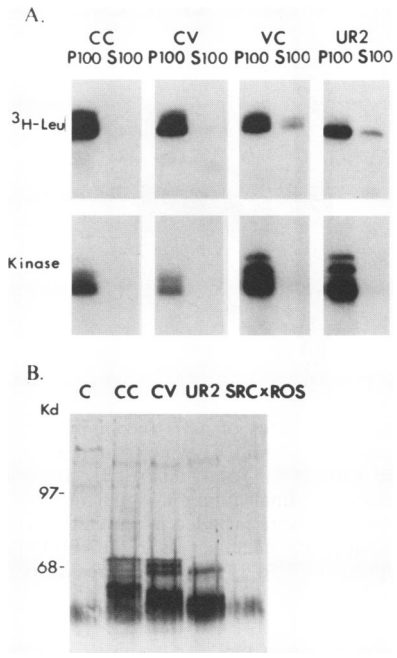


FIG. 8. Membrane association of the recombinant c-*ros* virus proteins. (A) Equal numbers of infected and control CEF labeled with [$^3$H]Leu were Dounce homogenized, and the extracts were separated into membrane-rich P100 and cytosolic S100 fractions by differential centrifugation. Aliquots of each fraction were analyzed by direct immunoprecipitation with anti-Ros (top) or by in vitro kinase assay following immunoprecipitation (bottom). (B) Cell surface localization of the viral proteins was detected by biotin labeling and chemiluminescence detection as described in Materials and Methods. Normal and infected CEF were transferred and seeded at a density of about 5 × 10$^6$ cells per 10-cm-diameter dish 1 day prior to the experiment. SRC × ROS encodes an nonprotruding membrane-associated Src-Ros chimera protein (23) and was included as a control for demonstrating intactness of the membrane and nonpermeability of biotin during the treatment. CC, CV, and VC represent CC5d, CV5d, and VCros, respectively.

Potential substrates of c-*ros* chimera proteins and UR2 P68$^{gag\text{-}ros}$ were compared by $^{32}P_i$ labeling (data not shown) and Western blotting (Fig. 9) with using various anti-P-Tyr antisera. Both types of experiments showed that there were distinctive P-Tyr protein patterns for cells infected with CC5d and CV5d versus UR2 or VCros. A tyrosine-phosphorylated

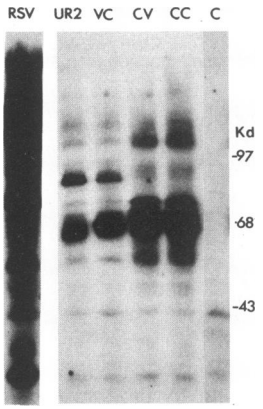


FIG. 9. Cellular substrates of c-*ros* recombinant proteins. Equal numbers of infected or control CEF were treated for 12 h with 50 μM vanadate before extraction. Total unlabeled protein extracts were analyzed by Western blotting with a polyclonal anti-P-Tyr serum (23). The RSV-infected CEF were included in parallel for comparison and also for demonstrating the effectiveness of the anti-P-Tyr serum. CC, CV, and VC represent CC5d, CV5d, and VCros, respectively.

protein band of about 88 kDa detected in UR2- and VCros-infected cells was not seen in CC5d- and CV5d-infected cells. Instead, proteins of 60, 75, and 120 to 140 kDa were more prominent in CC5d- and CV5d-infected cells than in UR2- and VCros-infected cells. Similar results were obtained with use of monoclonal anti-P-Tyr antibodies PY20 and 4G10 (data not shown). Compared with RSV-transformed cells, *ros*-transformed cells contain much less P-Tyr proteins, confirming our previous observation for the RPTK versus cytoplasmic PTK oncogenes (23). The result for RSV-infected cells (Fig. 9) also demonstrated the capability of our polyclonal anti-P-Tyr serum to recognize efficiently the P-Tyr proteins. Therefore, differential phosphorylation of cellular proteins represents the only biochemical property found to be different among the CC5d and CV5d versus UR2 and VCros proteins; however, the biological significance of those differentially phosphorylated proteins remains to be elucidated.

## DISCUSSION

Our data show that native or 5′ internally deleted c-*ros* protein is unable to transform CEF. A native RPTK normally requires ligand binding for its activation. Addition of the ligand to cells overexpressing an RPTK or coexpression of the RPTK and its cognate ligand is usually required to promote cell transformation. Therefore, it is not surprising that expression of native c-*ros* cannot lead to cell transformation. Its low abundance of expression and weak kinase activity most likely account for its lack of cell transformation ability. Internal deletion of 1,661 aa in the EC domain appears to constitutively activate the c-*ros*, as the ppcros protein is expressed in COS cells (Fig. 3) and CEF (data not shown) has a kinase activity indistinguishable from that of UR2 v-*ros*. The ppcros protein is very stable, membrane bound, and expressed on the cell surface (data not shown) as is the UR2 P68$^{gag\text{-}ros}$. The reason for its failure to transform CEF is currently unclear.

Our results also indicate that 5′ truncation and joining of the remaining 3′ region of c-*ros* to viral *gag* as in CCros and CVros is insufficient to activate the cell-transforming potential irrespective of the 3′ sequence alteration. However, this potential can be manifested if the sequence immediately upstream of the TM domain is deleted. This result corroborates our previous observation for IR (35) and IGFR (26, 27). In those studies, we found that deletion of the sequence immediately upstream of the TM domain of the Gag-IR and Gag-IGFR fusion proteins resulted in enhancement of their cell-transforming activity and activation of tumorigenicity. The current result further strengthens our hypothesis that sequences immediately upstream of the TM domains of these related RPTKs have a negative effect on their transforming potency. In the cases of Gag-IR and Gag-IGFR, relief of this negative effect was correlated with a severalfold increase of their PTK activity. Deletion of the EC sequences upstream of the TM domain of CCros and CVros results in greatly increased abundance, stability, efficiency of membrane association, and kinase activity of CC5d and CV5d proteins. The reason for the negative effect of the EC sequence on the CCros and CVros proteins is unclear. We speculate that the sequence immediately upstream of the TM domain has a modulatory effect on the conformation and signal transduction of an RPTK. In the cases of epidermal growth factor and platelet-derived growth factor receptors, ligand binding has been shown to trigger oligomerization and activation of these receptors (43). For IR and IGFR, in which the resting receptors already exist as dimeric molecules (10, 42), ligand binding was proposed to further stabilize the complex and activate the kinase activity (43). However, none of those models excludes the possibility that the extracellular signal can be transmitted through the receptor molecule via conformational changes or may affect interaction of the receptor with some other membrane protein(s). Sequences immediately upstream and downstream of the TM domain could be involved in controlling those changes and/or interaction. It has been shown that mutations of certain amino acids, particularly the positively charged residues, in the vicinity of the TM domain of a TM molecule could drastically affect its membrane-anchoring stability and even revert its membrane orientation (19, 33). Deletion of the sequences immediately upstream of the TM domains of the CCros and CVros proteins may release the physical constraint of these TM molecules and render them constitutively active in kinase activity.

Sequencing of CC5d and CV5d reveals that they have the same *gag-ros* junction as does the UR2 v-*ros*, apparently resulting from deletion mediated by the 21-nucleotide repeats present in the CCros and CVros constructs, leaving only one copy of the repeat (Fig. 1B). This finding is consistent with a model that we proposed previously for the generation of *src* deletion mutants during reverse transcription (34) and is also consistent with the observation of reproducible generation of the CC5d and CV5d from independent transfection experiments with CCros and CVros as well as the identity of deletion junction in independent PCR clones of the CC5d and CV5d DNAs. The fact that it requires 4 to 5 weeks or five to six passages to select and amplify the transforming CC5d and CV5d variants indicates that the parental CCros and CVros are nontransforming. The direct repeats apparently promoted the deletion event. Without them, a longer period of time for the generation of transforming variants would most likely be required and the variants would likely to be heterogeneous in their deletions.

The VCros virus is as potent as UR2 (VVros), whereas CC5d is only weakly transforming and tumorigenic. The apparent difference between the two is the 3-aa insertion in the TM domain. This result suggests that the 3-aa insertion in the TM domain may have a profound positive effect on the biological activity of the VCros and UR2 proteins. However, at present, we cannot exclude the possibility that some additional

TABLE 2. Summary of the biological and biochemical properties of various c-*ros* and v-*ros* variants

| Virus | Transforming activity | | Properties of *ros* proteins | | | |
|---|---|---|---|---|---|---|
| | In vitro[a] | In vivo[b] | Kinase activity[c] | Membrane association[d] | Surface localization[e] | $T_{1/2}$[f] (h) |
| Ufcros | − | ND | + | ++ | ND | 1 |
| Uppcros | − | ND | ++++ | ++++ | Yes | 8 |
| UR2 | ++++ | ++++ | ++++ | ++++ | Yes | 1,1.5–2.0 |
| VCros | ++++ | ++++ | ++++ | ++++ | Yes | 1 |
| CCros | − | ND | + | ++ | ND | 0.5 |
| CVros | − | ND | + | ++ | ND | 0.75 |
| CC5d | + | + | ++++ | ++++ | Yes | 2.5 |
| CV5d | + | +++ | ++++ | ++++ | Yes | 1.5 |

[a] CEF-transforming potential as measured by morphological changes and colony-forming ability of the infected cells as represented by the data shown in Fig. 5.
[b] Tumorigenicity in newly hatched chicks as shown in Table 1. Those with no CEF-transforming activity were not tested for tumorigenicity (ND).
[c] In vitro activity in autophosphorylation and phosphorylation of the added exogenous substrate as shown in Fig. 3, 4, and 6, as well as the ability to promote tyrosine phosphorylation of cellular proteins in the infected or transfected cells as illustrated in Fig. 9 and other data not shown.
[d] Cofractionation with the P100 fractions as shown in Fig. 3, 4, and 8 and other data not shown.
[e] Assessed by biotin labeling as illustrated in Fig. 8 and additional data for ppcros and VCros proteins not shown. Because of the very low level expression of fcros, CCros, and CVros proteins, their surface localization analysis by biotin labeling was not successful.
[f] Determined by pulse-chase labeling as shown in Fig. 3, 4, and 7 and additional data for the ppcros protein not shown. Half-lives of the UR2 v-*ros* protein were estimated to be about 1 h in CEF and 1.5 to 2.0 h in COS cells, as shown in Fig. 7 and 4, respectively.

mutation(s) is present in CC5d and CV5d which has a down-modulatory effect. A single charged amino acid mutation in the TM domain of the proto-oncogene *neu* is responsible for its oncogenic activation (1). However, none of the additional 3 aa in the TM domains of VCros and UR2 is charged. It would be interesting to determine how deletion of the 3 aa from UR2 $P68^{gag\text{-}ros}$ would affect its biochemical and biological properties.

A comparison of CC5d and CV5d indicates that the 3′-end alteration has only a mild enhancing effect on in vitro cell-transforming activity. Surprisingly, CV5d is nearly as potent as UR2 and VCros in tumorigenicity. Further mutation(s) of CV5d in vivo could be responsible for the observed tumorigenicity. The carboxyl alterations in CV5d may have enhanced this propensity, since CC5d appears unable to attain potent tumorigenicity through mutation(s) as readily as CV5d can.

Whereas CC5d, CV5d, VCros, and UR2 display a wide spectrum of cell-transforming potency, the PTK activities of their encoded proteins appear to be indistinguishable (Table 2). This finding indicates that some factor(s) other than the kinase activity must play an important role in determining the transforming potency of an oncogenic PTK protein. Our data show that all of those *ros* proteins are membrane associated, expressed equally well on the surface, and equally capable of associating with PI3K (data not shown). CC5d and CV5d proteins have a longer half-life and higher steady-state level than those of VCros and UR2. The difference in P-Tyr substrate patterns in the CC5d- and CV5d-infected cells versus the VCros- and UR2-infected cells represents the only detectable difference among these viruses. The reason for this difference and its biological significance needs to be elucidated.

## ACKNOWLEDGMENTS

We thank R. Kohanski for the gift of purified lysozyme polypeptides and D. Liu for commenting on the manuscript.

This work was supported by NIH grant CA29339.

## REFERENCES

1. **Bargmann, C. I., M.-C. Huang, and R. A. Weinberg.** 1986. Multiple independent activation of the neu oncogene by a point mutation altering the transmembrane domain of P185. Cell **45**:649–657.
2. **Birchmeier, C., D. Burnbaum, G. Waitches, O. Fasano, and M. Wigler.** 1986. Characterization of an activated human *ros* gene. Mol. Cell. Biol. **6**:1122–1129.
3. **Birchmeier, C., K. O'Neill, M. Riggs, and M. Wigler.** 1990. Characterization of ROS1 cDNA from human glioblastoma cell line. Proc. Natl. Acad. Sci. USA **87**:4799–4803.
4. **Birchmeier, C., S. Sharma, and M. Wigler.** 1987. Expression and rearrangement of the ROS1 gene in human glioblastoma cells. Proc. Natl. Acad. Sci. USA **84**:9270–9274.
5. **Chen, J., D. Heller, B. Poon, L. Kang, and L.-H. Wang.** 1991. The proto-oncogene c-*ros* codes for a transmembrane tyrosine protein kinase sharing sequence and structure homology with sevenless protein of *Drosophila melanogaster*. Oncogene **6**:257–264.
6. **Chen, J., C. S. Zong, and L.-H. Wang.** Restricted expression of chicken proto-oncogene c-*ros* in the epithelial cells of different organs suggests that it may play roles in both development and mature function. Submitted for publication.
7. **Coussens, L., C. Van Beveren, D. Smith, E. Chen, R. L. Mitchell, C. M. Isake, I. M. Verma, and A. Ullrich.** 1986. Structure alteration of viral homologue of receptor proto-oncogene fms at carboxyl terminus. Nature (London) **320**:277–280.
8. **Ebina, Y., L. Ellis, K. Larnajin, M. Edery, L. Graf, E. Clauser, J.-H. Ou, F. Masiarz, Y. W. Kan, I. D. Goldfine, R. A. Roth, and W. J. Rutter.** 1985. The human insulin receptor cDNA; the structural basis for hormone-activated transmembrane signalling. Cell **40**:747–758.
9. **Ellis, L., E. Clouser, D. O. Morgan, M. Edery, and R. A. Roth.** 1986. Replacement of insulin receptor tyrosine residues 1162 and 1163 compromises insulin stimulated kinase activity and uptake of 2-deoxyglucose. Cell **45**:721–732.
10. **Ellis, L., D. O. Morgan, E. Clauser, M. Edery, S.-M. Jong, L.-H. Wang, R. A. Roth, and W. J. Rutter.** 1986. Mechanism of receptor mediated transmembrane communication. Cold Spring Harbor Symp. Quant. Biol. **51**:773–784.
11. **Feldman, R. A., L.-H. Wang, H. Hanafusa, and P. C. Balduzzi.** 1982. Avian sarcoma virus UR2 encodes a transforming protein which is associated with a unique protein kinase activity. J. Virol. **42**:228–236.
12. **Fukui, Y., S. Kornbluth, S.-M. Jong, L.-H. Wang, and H. Hanafusa.** 1989. Phosphatidylinositol kinase type I activity associated with various oncogenes products. Oncogene Res. **4**:283–292.
13. **Garber, E. A., T. Hanafusa, and H. Hanafusa.** 1985. Membrane association of the transforming protein of avian sarcoma virus UR2 and mutants temperature sensitive for cellular transformation and protein kinase activity. J. Virol. **56**:790–797.
14. **Graham, F. L., and A. J. van der Eb.** 1973. A new technique for the assay of infectivity of human adenovirus DNA. Virology **521**:456–467.
15. **Hafen, E., K. Basler, J.-E. Edstrom, and G. M. Rubin.** 1987. Sevenless, a cell-specific homeotic gene of *Drosophila*, encodes a

putative transmembrane receptor with a tyrosine kinase domain. Science **236**:55–63.
16. **Hamaguchi, M., C. Grandori, and H. Hanafusa.** 1988. Phosphorylation of cellular proteins in Rous sarcoma virus-infected cells: analysis by use of anti-phosphotyrosine antibodies. Mol. Cell. Biol. **8**:3035–3042.
17. **Hampe, A., M. Gobert, C. J. Sherr, and F. Galibert.** 1984. Nucleotide sequence of the feline retrovirus oncogene v-*fms* shows an unexpected homology with oncogenes encoding tyrosine specific protein kinases. Proc. Natl. Acad. Sci. USA **81**:85–89.
18. **Hanafusa, H.** 1969. Rapid transformation of cells by Rous sarcoma virus. Proc. Natl. Acad. Sci. USA **63**:318–325.
19. **Hunter, E.** 1988. Membrane insertion and transport of viral glycoproteins: a mutational analysis, p. 109–158. *In* R. C. Das and R. W. Robbins (ed.), protein transfer and organelle biogenesis. Academic Press, San Diego, Calif.
20. **Jong, S.-M. J., and L.-H. Wang.** 1987. The transforming protein $p68^{gag\text{-}ros}$ of avian sarcoma virus UR2 is a transmembrane protein with the *gag* portion protruding extracellularly. Oncogene Res. **1**:7–21.
21. **Jong, S.-M. J., and L.-H. Wang.** 1990. Role of Gag sequence in the biochemical properties and transforming activity of avian sarcoma virus UR2-encoded Gag-Ros fusion protein. J. Virol. **64**:5997–6009.
22. **Jong, S.-M. J., and L.-H. Wang.** 1991. Two point mutations in the transmembrane domain of $P68^{gag\text{-}ros}$ inactivate its transforming activity and cause a delay in membrane association. J. Virol. **65**:180–189.
23. **Jong, S.-M. J., C. S. Zong, T. Dorai, and L.-H. Wang.** 1992. Transforming properties and substrate specificity of the protein tyrosine kinase oncogenes *ros*, *src*, and their recombinants. J. Virol. **66**:4909–4918.
24. **Kawai, S., and M. Nishizawa.** 1984. New procedure for DNA transfection with polycation and dimethyl sulfoxide. Mol. Cell. Biol. **4**:1172–1174.
25. **Kohanski, R. A., and M. D. Land.** 1986. Kinetics evidence for activating and non-activating components of autophosphorylation of the insulin receptor protein kinase. Biochem. Biophy. Res. Commun. **134**:1312–1318.
26. **Liu, D., W. J. Rutter, and L.-H. Wang.** 1992. Enhancement of transforming potential of human insulinlike growth factor I receptor by N-terminal truncation and fusion to avian sarcoma virus UR2 *gag* sequence. J. Virol. **66**:374–385.
27. **Liu, D., W. J. Rutter, and L.-H. Wang.** 1993. Modulating effect of extracellular sequence of human insulinlike growth factor I receptor on its transforming and tumorigenic potential. J. Virol. **67**:9–18.
28. **Matsushime, H., L.-H. Wang, and M. Shibuya.** 1986. Human c-*ros*-1 gene homologous to the v-*ros* sequence of UR2 sarcoma virus encodes for a transmembrane receptor-like molecule. Mol. Cell. Biol. **6**:3000–3004.
29. **Matsushime, H., and M. Shibuya.** 1990. Tissue-specific expression of rat c-*ros-1* gene and a partial structural similarity of its predicted products with *sev* protein of *Drosophila melanogaster*. J. Virol. **64**:2117–2125.
30. **Neckameyer, W. S., M. Shibuya, M.-T. Hsu, and L.-H. Wang.** 1986. Proto-oncogene c-*ros* codes for a molecule with structural features common to those of growth factor receptors and displays tissue specific and developmentally regulated expression. Mol. Cell. Biol. **6**:1478–1486.
31. **Neckameyer, W. S., and L.-H. Wang.** 1985. Nucleotide sequencing of avian sarcoma virus UR2 and comparison of its transforming gene with other members of the tyrosine protein kinase oncogene family. J. Virol. **53**:879–884.
32. **Ng, D. T. W., S. W. Hiebert, and R. A. Lamb.** 1990. Different roles of individual N-linked oligosaccharide chains in folding, assembling, and transport of the simian virus 5 hemagglutinin-neuraminidase. Mol. Cell. Biol. **10**:1989–2001.
33. **Nielsen, I., and G. von Heijne.** 1990. Fine-tuning the topology of polytopic membrane proteins: role of positively and negatively charged amino acids. Cell **62**:1135–1141.
34. **Parvin, J. D., and L.-H. Wang.** 1984. Mechanism for the generation of *src*-deletion mutants and recovered sarcoma viruses: identification of viral sequences involved in *src* deletions and in recombination with c-*src* sequences. Virology **138**:236–245.
35. **Poon, B., D. Dixon, L. Ellis, R. A. Roth, W. J. Rutter, and L.-H. Wang.** 1991. Molecular basis of the activation of the tumorigenic potential of gag-insulin receptor chimeras. Proc. Natl. Acad. Sci. USA **88**:877–881.
36. **Sanger, F., S. Nicklen, and A. R. Coulson.** 1977. DNA sequence with chain-terminating inhibitors. Proc. Natl. Acad. Sci. USA **74**:5463–5467.
37. **Sonnenberg, E., A. Godecke, B. Walter, F. Bladt, and C. Birchmeier.** 1991. Transient and locally restricted expression of the *ros*1 proto-oncogene during mouse development. EMBO J. **10**:3693–3702.
38. **Takeya, T., R. A. Feldman, and H. Hanafusa.** 1982. DNA sequence of viral and cellular *src* gene of chickens. I. Complete nucleotide sequence of an *Eco*RI fragment of recovered avian sarcoma virus which codes for gp37 and $pp60^{src}$. J. Virol. **44**:1–11.
39. **Tessarollo, L., L. Nagarajan, and L. F. Parada.** 1992. c-*ros*: the vertebrate homolog of the *sevenless* tyrosine kinase receptor is tightly regulated during organogenesis in mouse embryonic development. Development **115**:11–20.
40. **Ullrich, A., J. R. Bell, E. Y. Chen, R. Herrera, L. M. Petruzzelli, T. J. Dull, A. Gray, L. Coussens, Y.-C. Liao, M. Tsubokawa, A. Mason, P. H. Seeburg, C. Grunfeld, O. M. Rosen, and J. Ramachandran.** 1985. Human insulin receptor and its relationship to the tyrosine kinase family of oncogenes. Nature (London) **313**:756–761.
41. **Ullrich, A., L. Coussens, J. S. Hayflick, T. J. Dull, A. W. Tam, J. Lee, Y. Yarden, T. A. Libermann, J. Schlessinger, J. Downward, E. L. V. Mayes, N. Whittle, M. D. Waterfield, and P. H. Seeburg.** 1984. Human epidermal growth factor receptor cDNA sequence and abundant expression of the amplified gene in A431 epidermoid carcinoma cells. Nature (London) **309**:418–425.
42. **Ullrich, A., A. Gray, A. W. Tam, T. Yang-Feng, M. Tsubokawa, C. Collins, W. Henzel, T. Le Bon, S. Kathuria, E. Chen, S. Jacobs, U. Francke, J. Ramachandran, and Y. Fujita-Yamaguchi.** 1986. Insulin-like growth factor I receptor primary structure—comparison with insulin receptor suggests structural determinants that define functional specificity. EMBO J. **5**:2503–2512.
43. **Ullrich, A., and J. Schlessinger.** 1990. Signal transduction by receptors with tyrosine kinase activity. Cell **61**:202–212.
44. **Wang, L.-H., F. Feldman, M. Shibuya, H. Hanafusa, M. F. D. Notter, and P. Balduzzi.** 1981. Genetic structure, transforming sequence, and gene product of avian sarcoma virus UR1. J. Virol. **40**:258–267.
45. **Wang, L.-H., H. Hanafusa, F. D. Notter, and P. C. Balduzzi.** 1982. Genetic structure and transforming sequence of avian sarcoma virus UR2. J. Virol. **41**:833–841.
46. **Woolford, J., A. McAuliffe, and L. R. Rohrschneider.** 1988. Activation of the feline c-fms proto-oncogene: multiple alterations are required to generate a fully transformed phenotypes. Cell **55**:965–977.
47. **Yarden, Y., J. A. Escohedo, W.-J. Kuang, T. L. Yang-Feng, T. O. Daniel, P. M. Tremble, E. Y. Chen, M. E. Ando, R. N. Harkins, U. Francke, V. A. Fried, A. Ullrich, and L. T. Williams.** 1986. Structure of the receptor of plate-derived growth factor helps to define a family of closely related growth factor receptors. Nature (London) **323**:226–232.